*Progress In Electromagnetics Research B, Vol. 24, 17–32, 2010*

# MAGNETIC FIELD CREATED BY A UNIFORMLY MAGNETIZED TILE PERMANENT MAGNET

**R. Ravaud and G. Lemarquand**

Laboratoire d'Acoustique de l'Universite du Maine
UMR CNRS 6613, Le Mans, France

**V. Lemarquand**

IUT
Universite de Toulouse
Figeac, France

**Abstract**—This paper presents a general analytical formulation for calculating the three-dimensional magnetic field distribution produced by Halbach structures with radial or axial polarization directions. Our model allows us to study tile permanent magnets of various magnetization directions and dimensions. The three magnetic field components are expressed in terms of analytical and semi-analytical parts using only one numerical integration. Consequently, the computational cost of our model is lower than 1 s for calculating the magnetic field in any point of space. All our expressions have been checked with previous analytical models published in the literature. Then, we present two optimized permanent magnet structures generating sinusoidal radial fields.

## 1. INTRODUCTION

This paper continues the work published in a previous paper [1]. We present a more general formulation of the magnetic field produced by a tile permanent magnet whose polarization can be directed along any direction of space. Such a formulation is suitable for studying MRI structures or more generally Halbach structures [2] using tile permanent magnets with radial or axial polarization directions. For MRI structures, it is well known that analytical expressions are suitable

*Received 22 June 2010, Accepted 20 July 2010, Scheduled 26 July 2010*
Corresponding author: G. Lemarquand (guy.lemarquand@ieee.org).

tools for optimizing the device dimensions to obtain the greatest static magnetic field [3–5].

Several approaches are commonly used for optimizing permanent magnet structures, these approaches are based on analytical [6, 7] or numerical methods [8]. Furthermore, some original methods have been proposed for designing MRI structures made of permanent magnets by employing inverse methods [9].

The other applications using tile permanent magnets are certainly the magnetic couplings [10–14] and the electric machines [15–18]. Indeed, the radial field in electric machines is obtained by stacking together tile permanent magnets with different polarizations. This radial field can be trapezoidal or sinusoidal. The easiest way of optimizing the radial field in electric machines is to use analytical formulations with a low computational cost.

The analytical method we use in this paper is based on the coulombian model of a magnet. This model implies the existence of fictitious magnetic charges located on the faces of a permanent magnet [19, 20]. Such an analytical method has been widely used by many authors for calculating the magnetic field produced by ring permanent magnets radially and axially magnetized [21–23]. It is to be noted that such an approach is suitable for studying Halbach structures [24], wigglers, electric machines and magnetic sensors [25].

The main goal of this paper is to present a general analytical formulation allowing the study of Halbach structures with radial or axial polarization directions. For instance, our model can be used for calculating the magnetic field produced by either the configuration shown in Fig. 1 or the one shown in Fig. 2. Then, we present two optimized structures generating a sinusoidal radial field in front of the magnets.

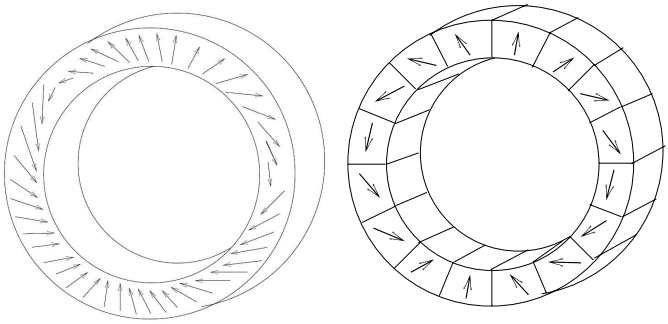

**Figure 1.** Halbach structure made of tile permanent magnets using radial polarization directions: left = ideal structure, right = real structure.

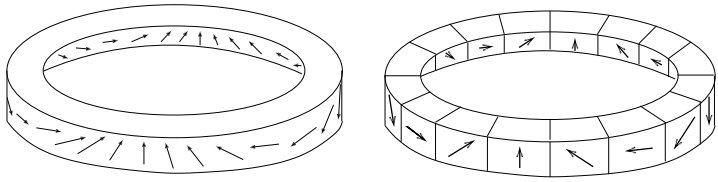

**Figure 2.** Halbach structure made of tile permanent magnets using axial polarization directions: left = ideal structure, right = real structure.

## 2. NOTATION AND GEOMETRY

The geometry considered is shown in Fig. 3. We consider a tile permanent magnet whose polarization is uniform. Its inner radius is $r_1$, its outer one is $r_2$. Its height is $z_2 - z_1$ and its angular width is $\theta_{j+1} - \theta_j$. The vector polarization of the tile permanent magnet shown in Fig. 3 is expressed as follows:

$$\vec{J} = J\cos(\theta_f)\sin(\phi)\vec{X} + J\sin(\theta_f)\sin(\phi)\vec{Y} + J\cos(\phi)\vec{Z} \tag{1}$$

The three vectors $\vec{X}$, $\vec{Y}$ and $\vec{Z}$ are linked to the global coordinate system $\vec{u}_x$, $\vec{u}_y$, $\vec{u}_z$:

$$\begin{aligned}
\vec{X} &= \cos\left(\frac{\theta_j + \theta_{j+1}}{2}\right)\vec{u}_x + \sin\left(\frac{\theta_j + \theta_{j+1}}{2}\right)\vec{u}_y \\
\vec{Y} &= -\sin\left(\frac{\theta_j + \theta_{j+1}}{2}\right)\vec{u}_x + \cos\left(\frac{\theta_j + \theta_{j+1}}{2}\right)\vec{u}_y \\
\vec{Z} &= \vec{u}_z
\end{aligned} \tag{2}$$

We also define the normal units of the tile permanent magnet as follows:

$$\begin{aligned}
\vec{n}_1 &= -\cos(\theta)\vec{u}_x - \sin(\theta)\vec{u}_y \\
\vec{n}_2 &= -\sin(\theta_{j+1})\vec{u}_x + \cos(\theta_{j+1})\vec{u}_y \\
\vec{n}_3 &= \cos(\theta)\vec{u}_x + \sin(\theta)\vec{u}_y \\
\vec{n}_4 &= \sin(\theta_j)\vec{u}_x - \cos(\theta_j)\vec{u}_y \\
\vec{n}_5 &= \vec{u}_z \\
\vec{n}_6 &= +\vec{u}_z
\end{aligned} \tag{3}$$

By using the previous relations, the vector polarization can be expressed as follows:

$$\begin{aligned}
\vec{J} \;=\; & J\sin(\phi)\cos\left(\theta_f + \frac{\theta_j + \theta_{j+1}}{2}\right)\vec{u}_x \\
& + J\sin(\phi)\sin\left(\theta_f + \frac{\theta_j + \theta_{j+1}}{2}\right)\vec{u}_y + J\cos(\phi)\vec{u}_z
\end{aligned} \tag{4}$$

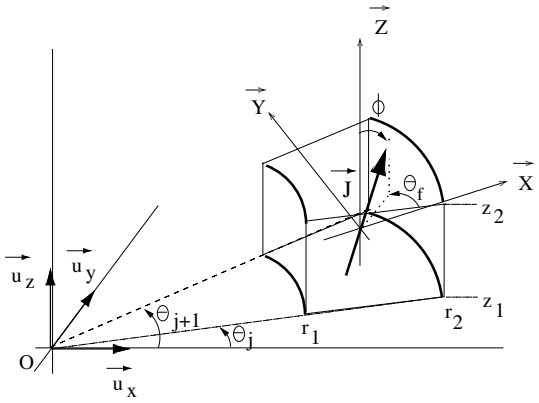


**Figure 3.** 3D representation of the geometry considered: a tile permanent magnet whose polarization is uniform.

The magnetic field produced by the tile permanent magnet is determined by using the Coulombian model. Consequently, this tile permanent magnet can be replaced by fictitious magnetic pole surface densities that are located on its faces (Fig. 4). These magnetic pole surface densities are determined by calculating the scalar product between the vector polarization $\vec{J}$ and the six normal units defined previously. We obtain the following results:

$$\begin{aligned}
\sigma_1(\theta) &= -J\sin(\phi)\cos\left[\theta - \left(\theta_f + \frac{\theta_j + \theta_{j+1}}{2}\right)\right] \\
\sigma_2 &= -J\sin(\phi)\sin\left[\theta_{j+1} - \left(\theta_f + \frac{\theta_j + \theta_{j+1}}{2}\right)\right] \\
\sigma_3(\theta) &= J\sin(\phi)\cos\left[\theta - \left(\theta_f + \frac{\theta_j + \theta_{j+1}}{2}\right)\right] \\
\sigma_4 &= J\sin(\phi)\sin\left[\theta_j - \left(\theta_f + \frac{\theta_j + \theta_{j+1}}{2}\right)\right] \\
\sigma_5 &= -J\cos(\phi) \\
\sigma_6 &= +J\cos(\phi)
\end{aligned} \tag{5}$$

The next step consists in calculating the three magnetic field components by using the previous fictitious magnetic pole surface densities.

## 3. ANALYTICAL MODEL OF THE MAGNETIC FIELD

This section presents the analytical model of the magnetic field created by a tile permanent magnet whose polarization is uniform. The magnetic field $\vec{H}(r,\theta,z)$ can be expressed in terms of three components. These three magnetic field components are determined in terms of cylindrical coordinates $H_r(r,\theta,z)$, $H_\theta(r,\theta,z)$ and $H_z(r,\theta,z)$.

The radial component of the magnetic field produced by the tile permanent magnet is expressed as follows;

$$\begin{aligned}
H_r(r,\theta,z) = & \frac{1}{4\pi\mu_0}\int_{\theta_j}^{\theta_{j+1}}\int_{z_1}^{z_2}\frac{\sigma_1\left(\tilde{\theta}\right)\left(r-r_2\cos\left(\theta-\tilde{\theta}\right)\right)r_2 d\tilde{\theta}d\tilde{z}}{\xi\left(r_2,\tilde{\theta},\tilde{z}\right)^3} \\
& +\frac{1}{4\pi\mu_0}\int_{\theta_j}^{\theta_{j+1}}\int_{z_1}^{z_2}\frac{\sigma_3\left(\tilde{\theta}\right)\left(r-r_1\cos\left(\theta-\tilde{\theta}\right)\right)r_1 d\tilde{\theta}d\tilde{z}}{\xi\left(r_1,\tilde{\theta},\tilde{z}\right)^3} \\
& +\frac{1}{4\pi\mu_0}\int_{\theta_j}^{\theta_{j+1}}\int_{r_1}^{r_2}\frac{\sigma_6\left(r-\tilde{r}\cos\left(\theta-\tilde{\theta}\right)\right)\tilde{r}d\tilde{\theta}d\tilde{r}}{\xi\left(\tilde{r},\tilde{\theta},z_2\right)^3} \\
& +\frac{1}{4\pi\mu_0}\int_{\theta_j}^{\theta_{j+1}}\int_{r_1}^{r_2}\frac{\sigma_5\left(r-\tilde{r}\cos\left(\theta-\tilde{\theta}\right)\right)\tilde{r}d\tilde{\theta}d\tilde{r}}{\xi\left(\tilde{r},\tilde{\theta},z_1\right)^3} \\
& +\frac{1}{4\pi\mu_0}\int_{r_1}^{r_2}\int_{z_1}^{z_2}\frac{\sigma_2\left(r-\tilde{r}\cos\left(\theta-\theta_{j+1}\right)\right)d\tilde{z}d\tilde{r}}{\xi\left(\tilde{r},\theta_{j+1},\tilde{z}\right)^3} \\
& +\frac{1}{4\pi\mu_0}\int_{r_1}^{r_2}\int_{z_1}^{z_2}\frac{\sigma_4\left(r-\tilde{r}\cos\left(\theta-\theta_j\right)\right)d\tilde{z}d\tilde{r}}{\xi\left(\tilde{r},\theta_j,\tilde{z}\right)^3}
\end{aligned} \tag{6}$$

where

$$\xi(\alpha,\beta,\gamma)=\sqrt{r^2+\alpha^2-2r\alpha\cos(\theta-\beta)+(z-\gamma)^2} \tag{7}$$

We obtain:

$$H_r(r,\theta,z)=H_r^{(I)}+H_r^{(II)}+H_r^{(III)} \tag{8}$$

$$H_r^{(I)}=\sum_{i=1}^{2}(-1)^i\int_0^{2\pi}\left\{\cos\left(\frac{\theta_j+\theta_{j+1}}{2}+\theta_f-\tilde{\theta}\right)\sin(\phi)\right\}(f(z_i)+g(z_i))d\tilde{\theta} \tag{9}$$

$$
\begin{aligned}
f(z_i) &= \frac{r_2(z_i - z)\beta(r_2, \tilde{\theta})}{\xi(r_2, z_i, \tilde{\theta})} \\
g(z_i) &= -\frac{r_1(z_i - z)\beta(r_1, \tilde{\theta})}{\xi(r_1, z_i, \tilde{\theta})} \\
\beta(a, c) &= \frac{r - a\cos(\theta - c)}{(r^2 + a^2 - 2ra\cos(\theta - c))}
\end{aligned}
\tag{10}
$$

$$
H_r^{(II)} = \sum_{i=1}^{2} (-1)^i \int_{r_1}^{r_2} \cos(\phi)\,(f(r_i) - g(r_i))\,d\tilde{\theta} \tag{11}
$$

$$
\begin{aligned}
f(r_i) =& \frac{-r_i\left(r^2 + 2(z - z_2)^2\cos(\theta - \tilde{\theta})\right)}{\xi(r_i, \tilde{\theta}, z_2)\left(-r^2 - 2(z - z_2)^2 + r^2\cos\left[2(\theta - \tilde{\theta})\right]\right)} \\
&+ \frac{\eta_2 - \eta_2\cos\left[2(\theta - \tilde{\theta})\right] + rr_i\cos\left[3(\theta - \tilde{\theta})\right]}{\xi(r_i, \tilde{\theta}, z_2)\left(-r^2 - 2(z - z_2)^2 + r^2\cos\left[2(\theta - \tilde{\theta})\right]\right)} \\
&- \cos(\theta - \tilde{\theta})\ln\left[r_i - r\cos(\theta - \tilde{\theta}) + \xi(r_i, \tilde{\theta}, z_2)\right] \\
g(r_i) =& \frac{r_i\left(r^2 + 2(z - z_1)^2\cos(\theta - \tilde{\theta})\right)}{\xi(r_i, \tilde{\theta}, z_1)\left(-r^2 - 2(z - z_1)^2 + r^2\cos\left[2(\theta - \tilde{\theta})\right]\right)} \\
&- \frac{\eta_1 - \eta_1\cos\left[2(\theta - \tilde{\theta})\right] + rr_i\cos\left[3(\theta - \tilde{\theta})\right]}{\xi(r_i, \tilde{\theta}, z_1)\left(-r^2 - 2(z - z_1)^2 + r^2\cos\left[2(\theta - \tilde{\theta})\right]\right)} \\
&+ \cos(\theta - \tilde{\theta})\ln\left[r_i - r\cos(\theta - \tilde{\theta}) + \xi(r_i, \tilde{\theta}, z_1)\right] \\
\eta_j =& r^2 + (z - z_j)^2
\end{aligned}
\tag{12}
$$

$$
H_r^{(III)} = \sum_{i=1}^{2} (-1)^i \int_{r_1}^{r_2} (d(\theta_{j+1}) - e(\theta_j))\,d\tilde{r} \tag{13}
$$

$$
\begin{aligned}
d(\theta_{j+1}) &= \frac{\tilde{r}(-z + z_i)(-r + \tilde{r}\cos(\theta - \theta_{j+1}))}{(r^2 + \tilde{r}^2 - 2r\tilde{r}\cos(\theta - \theta_{j+1}))\,\xi(\tilde{r}, \theta_{j+1}, z_i)}\,\frac{\sin(\phi)\sin\left[\frac{1}{2}(\theta_{j+1} - \theta_j - 2\theta_f)\right]}{} \\
e(\theta_j) &= \frac{\tilde{r}(z_i - z)(r - \tilde{r}\cos(\theta - \theta_j))}{(r^2 + \tilde{r}^2 - 2r\tilde{r}\cos(\theta - \theta_j))\,\xi(\tilde{r}, \theta_j, z_i)}\,\frac{\sin(\phi)\sin\left[\frac{1}{2}(\theta_j - \theta_{j+1} - 2\theta_f)\right]}{}
\end{aligned}
\tag{14}
$$

The azimuthal component of the magnetic field produced by the tile permanent magnet is expressed as follows;

$$\begin{aligned} H_\theta(r,\theta,z) &= \frac{1}{4\pi\mu_0}\int_{\theta_j}^{\theta_{j+1}}\int_{z_1}^{z_2}\frac{\sigma_1\left(\tilde{\theta}\right)\left(r_2\sin\left(\theta-\tilde{\theta}\right)\right)r_2 d\tilde{\theta}d\tilde{z}}{\xi\left(r_2,\tilde{\theta},\tilde{z}\right)^3} \\ &+\frac{1}{4\pi\mu_0}\int_{\theta_j}^{\theta_{j+1}}\int_{z_1}^{z_2}\frac{\sigma_3\left(\tilde{\theta}\right)\left(r_1\sin\left(\theta-\tilde{\theta}\right)\right)r_1 d\tilde{\theta}d\tilde{z}}{\xi\left(r_1,\tilde{\theta},\tilde{z}\right)^3} \\ &+\frac{1}{4\pi\mu_0}\int_{\theta_j}^{\theta_{j+1}}\int_{r_1}^{r_2}\frac{\sigma_6\left(\tilde{r}\sin\left(\theta-\tilde{\theta}\right)\right)\tilde{r}d\tilde{\theta}d\tilde{r}}{\xi\left(\tilde{r},\tilde{\theta},z_2\right)^3} \\ &+\frac{1}{4\pi\mu_0}\int_{\theta_j}^{\theta_{j+1}}\int_{r_1}^{r_2}\frac{\sigma_5\left(\tilde{r}\sin\left(\theta-\tilde{\theta}\right)\right)\tilde{r}d\tilde{\theta}d\tilde{r}}{\xi\left(\tilde{r},\tilde{\theta},z_1\right)^3} \\ &+\frac{1}{4\pi\mu_0}\int_{r_1}^{r_2}\int_{z_1}^{z_2}\frac{\sigma_2\left(\tilde{r}\sin\left(\theta-\theta_{j+1}\right)\right)d\tilde{z}d\tilde{r}}{\xi\left(\tilde{r},\theta_{j+1},\tilde{z}\right)^3} \\ &+\frac{1}{4\pi\mu_0}\int_{r_1}^{r_2}\int_{z_1}^{z_2}\frac{\sigma_4\left(\tilde{r}\sin\left(\theta-\theta_j\right)\right)d\tilde{z}d\tilde{r}}{\xi\left(\tilde{r},\theta_j,\tilde{z}\right)^3} \end{aligned} \tag{15}$$

The previous relation can be written in the following form:

$$H_\theta(r,\theta,z) = H_\theta^{(I)} + H_\theta^{(II)} + H_\theta^{(III)} \tag{16}$$

$$\begin{aligned} H_\theta^{(I)} = &\sum_{i=1}^{2}(-1)^i\frac{r_2^2(-z+z_i)\cos\left(\frac{\theta_j+\theta_{j+1}}{2}+\theta_f-\tilde{\theta}\right)\sin(\phi)\sin(\theta-\tilde{\theta})}{\xi(r_2,\tilde{\theta},z_i)\left(r^2+r_2^2-2rr_2\cos(\theta-\tilde{\theta})\right)} \\ &+\sum_{i=1}^{2}(-1)^i\frac{r_1^2(z-z_i)\cos\left(\frac{\theta_j+\theta_{j+1}}{2}+\theta_f-\tilde{\theta}\right)\sin(\phi)\sin(\theta-\tilde{\theta})}{\xi(r_1,\tilde{\theta},z_i)\left(r^2+r_1^2-2rr_1\cos(\theta-\tilde{\theta})\right)} \end{aligned} \tag{17}$$

By using $\theta_j = \theta_1$ and $\theta_{j+1} = \theta_2$, we have:

$$H_\theta^{(II)} = \sum_{i=1}^{2}\sum_{k=1}^{2}(-1)^k\left(fz_1 - f(z_2)\right) \tag{18}$$

$$\begin{aligned} f(z_i) &= -\frac{\cos(\phi)}{r}\left(\xi(r_i,z_1,\theta_k) + \eta\ln\left[r_i-\eta+\xi(r_i,z_1,\theta_k)\right]\right) \\ \eta &= r\cos(\theta-\theta_k) \end{aligned} \tag{19}$$

$$H_\theta^{(III)} = \int_{r_1}^{r_2} \left(m(\theta_{j+1}) - m(\theta_j)\right) d\tilde{r} \tag{20}$$

with

$$m(\alpha) = \sum_{i=1}^{2} (-1)^i \frac{\tilde{r^2}(-z+z_i)\sin(\phi)\sin(\theta-\alpha)\sin\left(\frac{1}{2}(\theta_j - \alpha + 2\theta_f)\right)}{(r^2+\tilde{r}^2-2r\tilde{r}\cos(\theta-\alpha))\xi(\tilde{r},\alpha,z_i)} \tag{21}$$

The axial component of the magnetic field produced by the tile permanent magnet is expressed as follows:

$$\begin{aligned}
H_z(r,\theta,z) = & \frac{1}{4\pi\mu_0}\int_{\theta_j}^{\theta_{j+1}}\int_{z_1}^{z_2} \frac{\sigma_1\left(\tilde{\theta}\right)(z-\tilde{z})\, r_2 d\tilde{\theta} d\tilde{z}}{\xi\left(r_2,\tilde{\theta},\tilde{z}\right)^3} \\
& + \frac{1}{4\pi\mu_0}\int_{\theta_j}^{\theta_{j+1}}\int_{z_1}^{z_2} \frac{\sigma_3\left(\tilde{\theta}\right)(z-\tilde{z})\, r_1 d\tilde{\theta} d\tilde{z}}{\xi\left(r_1,\tilde{\theta},\tilde{z}\right)^3} \\
& + \frac{1}{4\pi\mu_0}\int_{\theta_j}^{\theta_{j+1}}\int_{r_1}^{r_2} \frac{\sigma_6\,(z-z_2)\,\tilde{r} d\tilde{\theta} d\tilde{r}}{\xi\left(\tilde{r},\tilde{\theta},z_2\right)^3} \\
& + \frac{1}{4\pi\mu_0}\int_{\theta_j}^{\theta_{j+1}}\int_{r_1}^{r_2} \frac{\sigma_5\,(z-z_1)\,\tilde{r} d\tilde{\theta} d\tilde{r}}{\xi\left(\tilde{r},\tilde{\theta},z_1\right)^3} \\
& + \frac{1}{4\pi\mu_0}\int_{r_1}^{r_2}\int_{z_1}^{z_2} \frac{\sigma_2\,(z-\tilde{z})\, d\tilde{z} d\tilde{r}}{\xi\,(\tilde{r},\theta_{j+1},\tilde{z})^3} \\
& + \frac{1}{4\pi\mu_0}\int_{r_1}^{r_2}\int_{z_1}^{z_2} \frac{\sigma_4\,(z-\tilde{z})\, d\tilde{z} d\tilde{r}}{\xi\,(\tilde{r},\theta_j,\tilde{z})^3}
\end{aligned} \tag{22}$$

The previous relation can be reduced to the following form:

$$H_z(r,\theta,z) = H_z^{(I)} + H_z^{(II)} + H_z^{(III)} \tag{23}$$

$$H_z^{(I)} = \sum_{i=1}^{2}(-1)^i \int_0^{2\pi} \cos\left(\frac{\theta_j+\theta_{j+1}}{2} + \theta_f - \tilde{\theta}\right)\sin(\phi)\left(f(z_i)+g(z_i)\right) d\tilde{\theta} \tag{24}$$

with

$$\begin{aligned}
f(z_i) &= \frac{r_2}{\xi(r_2,\tilde{\theta},z_i)} \\
g(z_i) &= -\frac{r_1}{\xi(r_1,\tilde{\theta},z_i)}
\end{aligned} \tag{25}$$

$$H_z^{(II)} = \int_0^{2\pi} (h_z)\, d\tilde{\theta} \tag{26}$$

with

$$\begin{aligned} h_z = & \sum_{i=1}^{2} (-1)^i \frac{2\,(z-z_2)\cos(\phi)\left(r^2+(z-z_2)^2 - rr_i\cos\left(\theta-\tilde{\theta}\right)\right)}{\xi\left(r_i,\tilde{\theta},z_2\right)\left(-r^2-2\,(z-z_2)^2+r^2\cos\left[2\left(\theta-\tilde{\theta}\right)\right]\right)} \\ & + \sum_{i=1}^{2} (-1)^{i+1} \frac{2\,(z-z_1)\cos(\phi)\left(r^2+(z-z_1)^2 - rr_i\cos\left(\theta-\tilde{\theta}\right)\right)}{\xi\left(r_i,\tilde{\theta},z_1\right)\left(-r^2-2\,(z-z_1)^2+r^2\cos\left[2\left(\theta-\tilde{\theta}\right)\right]\right)} \end{aligned} \tag{27}$$

$$H_z^{(III)} = \sum_{i=1}^{2} (-1)^i \int_{r_1}^{r_2} \left(h_z(\theta_{j+1}) - h_z(\theta_j)\right) d\tilde{r} \tag{28}$$

with

$$\begin{aligned} h_z(\theta_{j+1}) &= \sum_{i=1}^{2} (-1)^i \frac{\tilde{r}\sin(\phi)\sin\left(\frac{1}{2}\left(\theta_j - \theta_{j+1} + 2\theta_f\right)\right)}{\xi\left(\tilde{r},\theta_{j+1},z_i\right)} \\ h_z(\theta_j) &= \sum_{i=1}^{2} (-1)^i \frac{\tilde{r}\sin(\phi)\sin\left(\frac{1}{2}\left(\theta_j - \theta_{j+1} + 2\theta_f\right)\right)}{\xi\left(\tilde{r},\theta_j,z_i\right)} \end{aligned} \tag{29}$$

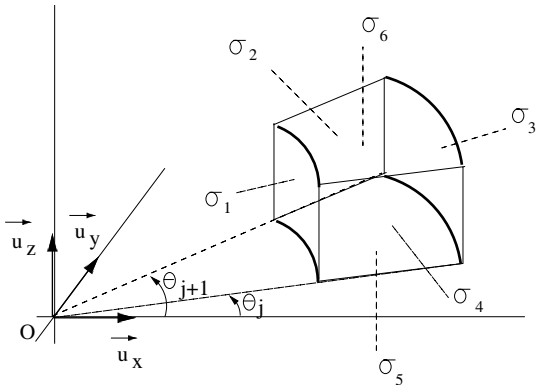


**Figure 4.** Definition of the fictitious magnetic pole surface densities $\sigma_1$, $\sigma_2$, $\sigma_3$, $\sigma_4$, $\sigma_5$ and $\sigma_6$.

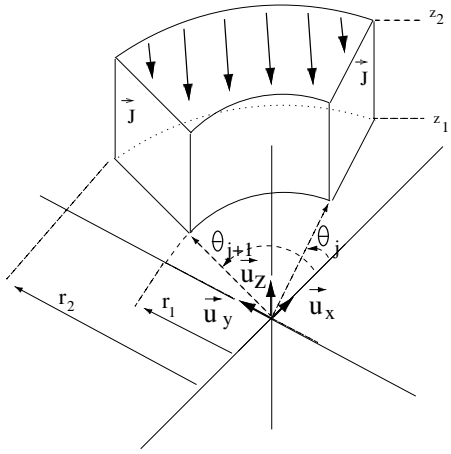


**Figure 5.** Structure considered for verifying the accuracy of our expressions.

## 4. VERIFICATION OF THE ACCURACY OF OUR ANALYTICAL EXPRESSIONS

This section presents a comparison of the three magnetic field components created by a tile permanent magnet whose polarization is both radial and uniform (as shown in Fig. 5). In other words, the vector polarization is defined as follows in that case:

$$\vec{J_p} = -J\cos\left(\frac{\theta_j + \theta_{j+1}}{2}\right)\vec{u}_x - J\sin\left(\frac{\theta_j + \theta_{j+1}}{2}\right)\vec{u}_y \qquad (30)$$

We have represented in Fig. 6 the radial field created by a tile permanent magnet whose polarization is $\vec{J_p}$ with our model and the one published in [1]. We have taken the following dimensions: $r_1 = 0.01\,\text{m}$, $r_2 = 0.015\,\text{m}$, $\theta_j = 0\,\text{rad}$, $\theta_{j+1} = \frac{\pi}{4}\,\text{rad}$, $z_1 = 0\,\text{m}$, $z_2 = 0.003\,\text{m}$, $\theta = \frac{\pi}{8}\,\text{rad}$, $\theta_f = 0\,\text{rad}$, $\phi = \frac{\pi}{2}\,\text{rad}$, $z = 0.0015\,\text{m}$. The Fig. 6 shows that our model is consistent with the one published in [1]. Furthermore, the Fig. 6 shows a dissymmetry of the radial field shape, which is consistent with the demagnetizing field in arc-shaped permanent magnets with small dimensions.

We have represented in Fig. 7 the azimuthal field created by a tile permanent magnet whose polarization is $\vec{J_p}$ with our model and the one published in [1]. We have taken the following dimensions: $r_1 = 0.025\,\text{m}$, $r_2 = 0.03\,\text{m}$, $\theta_j = 0\,\text{rad}$, $\theta_{j+1} = \frac{\pi}{4}\,\text{rad}$, $z_1 = 0\,\text{m}$, $z_2 = 0.003\,\text{m}$, $\theta_f = \pi\,\text{rad}$, $\phi = \frac{\pi}{2}\,\text{rad}$, $r = 0.022\,\text{m}$, $z = 0.001\,\text{m}$.

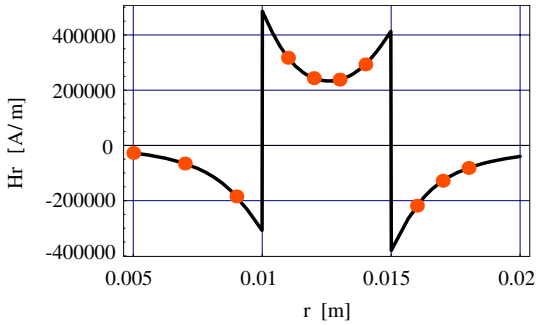


**Figure 6.** Representation of the radial field produced by a tile permanent magnet uniformly magnetized versus the radial direction ($r_1 = 0.01\,\mathrm{m}$, $r_2 = 0.015\,\mathrm{m}$, $\theta_j = 0\,\mathrm{rad}$, $\theta_{j+1} = \frac{\pi}{4}\,\mathrm{rad}$, $z_1 = 0\,\mathrm{m}$, $z_2 = 0.003\,\mathrm{m}$, $\theta = \frac{\pi}{8}\,\mathrm{rad}$, $\theta_f = \pi\,\mathrm{rad}$, $\phi = \frac{\pi}{2}\,\mathrm{rad}$, $z = 0.0015\,\mathrm{m}$).

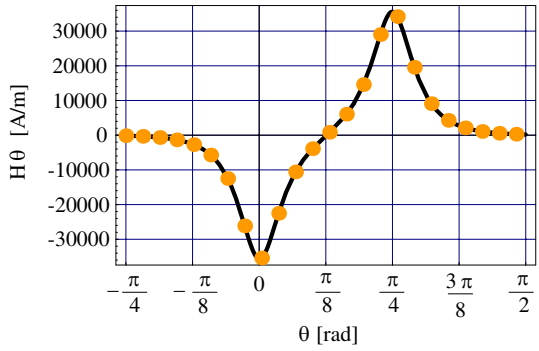


**Figure 7.** Representation of the azimuthal field produced by a tile permanent magnet uniformly magnetized.

The Fig. 7 also demonstrates that our model is consistent with the one published in [1].

Eventually, we have represented in Fig. 8 the axial field created by a tile permanent magnet whose polarization is $\vec{J}_p$ with our model and the one published in [1]. We have taken the following dimensions: $r_1 = 0.025\,\mathrm{m}$, $r_2 = 0.03\,\mathrm{m}$, $\theta_j = 0\,\mathrm{rad}$, $\theta_{j+1} = \frac{\pi}{4}\,\mathrm{rad}$, $z_1 = 0\,\mathrm{m}$, $z_2 = 0.003\,\mathrm{m}$, $\theta_f = \pi\,\mathrm{rad}$, $\phi = \frac{\pi}{2}\,\mathrm{rad}$, $r = 0.0249\,\mathrm{m}$. Fig. 8 also demonstrates that our model is consistent with the one published in [1].

As a remark, there is a difficulty in evaluating the magnetic field very near the magnet surface when the Green's function becomes singular. In that case, we use the Cauchy's principal value between the upper and lower surfaces of the magnet faces.

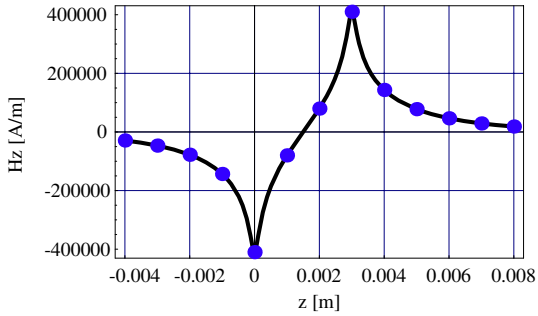


**Figure 8.** Representation of the axial field produced by a tile permanent magnet uniformly magnetized versus the axial direction ($r_1 = 0.025\,\mathrm{m}$, $r_2 = 0.03\,\mathrm{m}$, $\theta_j = 0\,\mathrm{rad}$, $\theta_{j+1} = \frac{\pi}{4}\,\mathrm{rad}$, $z_1 = 0\,\mathrm{m}$, $z_2 = 0.003\,\mathrm{m}$, $\theta_f = \pi\,\mathrm{rad}$, $\phi = \frac{\pi}{2}\,\mathrm{rad}$, $r = 0.0249\,\mathrm{m}$).

## 5. OBTAINING OPTIMIZED CONFIGURATIONS

This section illustrates the utility of using our analytical formulation for obtaining a sinusoidal radial field in an electric machine. Such a radial field can be obtained by using tile permanent magnets of various magnetization directions. We study two configurations. Basically, the first configuration consists of tile permanent magnets of various angular widths and the magnetic polarization directions are fixed. In other words, we have tile permanent magnets with radial and orthoradial polarizations and we look for the optimal angular widths so as to obtain a sinusoidal radial field in the air gap of the device. Such an optimization can be carried out by using a classical gradient method since the computational cost of our model is low. To do such an optimization, we have used the following device dimensions: $r_1 = 0.1\,\mathrm{m}$, $r_2 = 0.15\,\mathrm{m}$, $J = 1\,\mathrm{T}$, $z_1 = 0\,\mathrm{m}$, $z_2 = 0.03\,\mathrm{m}$, $r = 0.06\,\mathrm{m}$, $z = 0.015\,\mathrm{m}$, the largest angular width is $\frac{\pi}{3}\,\mathrm{rad}$ and the other one is $\frac{\pi}{6}\,\mathrm{rad}$. We have compared the obtained simulation with a simple radial field whose equation is $H_r(\theta) = 55\sin(2(\theta - 1.25))\,\mathrm{kA/m}$. The two simulations clearly show that we have succeeded in obtaining a sinusoidal radial field with the considered geometry.

The second configuration consists of a device made of tile permanent magnets with various polarization directions. In other words, all the tile permanent magnets have various angular widths and polarization directions. In this configuration, we look for the optimal angular widths and polarization directions so as to obtain a sinusoidal radial field in the air gap of the device. To do so, we have used the following device dimensions: $r_1 = 0.1\,\mathrm{m}$, $r_2 = 0.15\,\mathrm{m}$,

$J = 1\,\mathrm{T}$, $z_1 = 0\,\mathrm{m}$, $z_2 = 0.03\,\mathrm{m}$, $r = 0.05\,\mathrm{m}$, $z = 0.015\,\mathrm{m}$, the smallest angular width is $\frac{0.84\pi}{6}$ rad, the greatest angular width is $\frac{1.08\pi}{6}$ rad. As previously, we have compared the obtained simulation with a simple radial field whose equation is $H_r(\theta) = 60\sin(2(\theta - 1))\,\mathrm{kA/m}$.The two simulations clearly show that we have succeeded in obtaining a sinusoidal radial field with the considered geometry.

More generally, the Figs. 9 and 10 emphasize the utility of using analytical tools. Indeed, the computational cost for representing

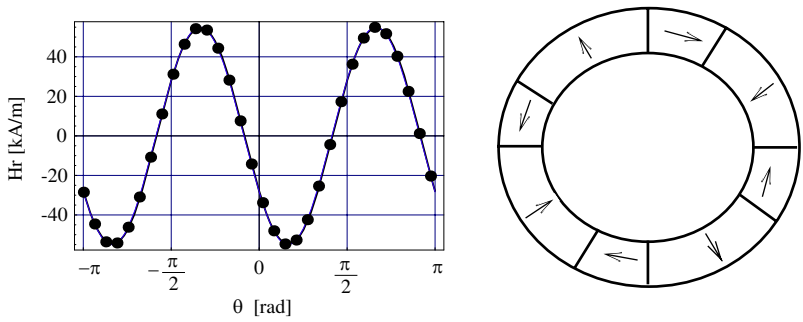


**Figure 9.** Representation of the sinusoidal radial field created by an optimized structure versus the angular direction; $r_1 = 0.1\,\mathrm{m}$, $r_2 = 0.15\,\mathrm{m}$, $J = 1\,\mathrm{T}$, $z_1 = 0\,\mathrm{m}$, $z_2 = 0.03\,\mathrm{m}$, $r = 0.05\,\mathrm{m}$, $z = 0.015\,\mathrm{m}$, the largest angular width is $\frac{\pi}{3}$ rad and the other one is $\frac{\pi}{6}$ rad, line = this work, points = $H_r(\theta) = 55\sin(2(\theta - 1.25))\,\mathrm{kA/m}$.

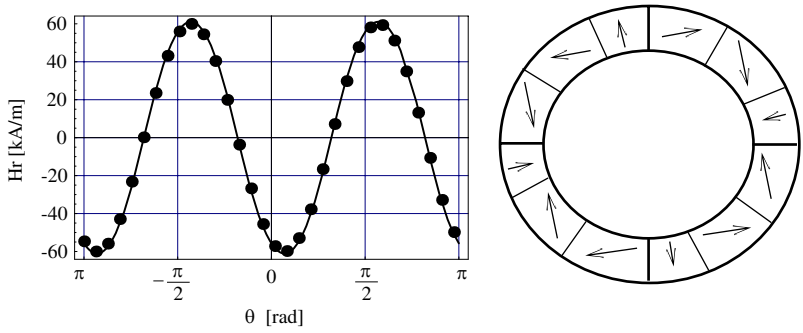


**Figure 10.** Representation of the sinusoidal radial field created by an optimized structure versus the angular direction; $r_1 = 0.1\,\mathrm{m}$, $r_2 = 0.15\,\mathrm{m}$, $J = 1\,\mathrm{T}$, $z_1 = 0\,\mathrm{m}$, $z_2 = 0.03\,\mathrm{m}$, $r = 0.05\,\mathrm{m}$, $z = 0.015\,\mathrm{m}$; line = this work, points = $H_r(\theta) = 60\sin(2(\theta - 1))\,\mathrm{kA/m}$, the smallest angular width is $\frac{0.84\pi}{6}$ rad, the greatest angular width is $\frac{1.08\pi}{6}$ rad.

this sinusoidal radial field is 3 s for the two previous simulations. Consequently, this is a suitable tool that can be used with any algorithm method so as to optimize the radial field in the air gap of the device.

## 6. CONCLUSION

This paper has presented analytical expressions of the magnetic field created by a tile permanent magnet uniformly magnetized. Our analytical expressions have a low computational cost and are presented in terms of analytical and semi-analytical parts. Basically, our expressions are sufficiently general to be used in many engineering applications like electric machines, couplings, wigglers or MRI devices. All our expressions have been compared to previous ones published in the literature. Eventually, we have presented two optimized configurations generating a sinusoidal radial field in the air gap of the device.

## REFERENCES

1. Ravaud, R., G. Lemarquand, and V. Lemarquand, "Magnetic field in MRI yokeless devices: Analytical approach," *Progress In Electromagnetics Research*, Vol. 94, 327–341, 2009.
2. Halbach, K., "Strong rare earth cobalt quadrupoles," *IEEE Trans. Magn.*, Vol. 26, No. 3, 3882–3884, 1979.
3. Marble, A. E., "Strong, stray static magnetic fields," *IEEE Trans. Magn.*, Vol. 44, No. 5, 576–580, 2008.
4. Chang, W., K. Chen, and L. Hwang, "Single-sided mobile NMR with a halbach magnet," *Magnetic Resonance Imaging*, Vol. 24, No. 8, 1095–1102, 2006.
5. Chen, J. and C. Xu, "An improved discrete configuration of a cylinder magnet for portable nuclear magnetic resonance instruments," *J. Appl. Phys.*, Vol. 101, No. 12, 2007.
6. Marble, A. E., I. V. Mastikhui, B. G. Colpitts, and B. J. Balcom, "Designing static fields for unilateral magnetic resonance by a scalar potential approach," *IEEE Trans. Magn.*, Vol. 43, No. 5, 1903–1911, 2007.
7. Jian, L. and K. T. Chau, "Analytical calculation of magnetic field distribution in coaxial magnetic gears," *Progress In Electromagnetics Research*, Vol. 92, 1–16, 2009.
8. Ryu, J. S., Y. Yao, C. S. Koh, and Y. J. Shin, "Development of

permanent magnet assembly for mri devices," *IEEE Trans. Magn.*, Vol. 42, No. 4, 1351–1353, 2006.

9. Thompson, M. R., R. W. Brown, and V. C. Srivastava, "An inverse approach to the design of mri main magnets," *IEEE Trans. Magn.*, Vol. 30, No. 1, 108–112, 1994.
10. Baran, W. and M. Knorr, "Synchronous couplings with SmCo5 magnets," *2nd Int. Workshop on RECo Permanent Magnets and Their Applications*, 140–151, Dayton, Ohio, USA, 1976.
11. Furlani, E. P., "Analysis and optimization of synchronous couplings," *J. Appl. Phys.*, Vol. 79, 4692–4694, 1996.
12. Elies, P. and G. Lemarquand, "Analytical study of radial stability of permanent magnet synchronous couplings," *IEEE Trans. Magn.*, Vol. 35, No. 4, 2133–2136, 1999.
13. Ravaud, R. and G. Lemarquand, "Magnetic couplings with cylindrical and plane air gaps: Influence of the magnet polarization direction," *Progress In Electromagnetics Research B*, Vol. 16, 333–349, 2009.
14. Ravaud, R., G. Lemarquand, V. Lemarquand, and C. Depollier, "Permanent magnet couplings: Field and torque three-dimensional expressions based on the coulombian model," *IEEE Trans. Magn.*, Vol. 45, No. 4, 1950–1958, 2009.
15. Wang, J., G. W. Jewell, and D. Howe, "Design optimisation and comparison of permanent magnet machines topologies," *IEE. Proc. Elect. Power Appl.*, Vol. 148, 456–464, 2001.
16. Furlani, E. P., "Computing the field in permanent-magnet axialfield motors," *IEEE Trans. Mag.*, Vol. 30, No. 5, 3660–3663, 1994.
17. Furlani, E. P., "Field analysis and optimization of NdFeB axial field permanent magnet motors," *IEEE Trans. Magn.*, Vol. 33, No. 5, 3883–3885, 1997.
18. Marinescu, M. and N. Marinescu, "New concept of permanent-magnet excitation for electrical machines," *IEEE Trans. Magn.*, Vol. 28, 1390–1393, 1992.
19. Babic, S. I., C. Akyel, and M. M. Gavrilovic, "Calculation improvement of 3D linear magnetostatic field based on fictitious magnetic surface charge," *IEEE Trans. Magn.*, Vol. 36, No. 5, 3125–3127, 2000.
20. Furlani, E. P., *Permanent Magnet and Electromechanical Devices: Materials, Analysis and Applications*, Academic Press, 2001.
21. Ravaud, R. and G. Lemarquand, "Comparison of the coulombian and amperian current models for calculating the magnetic field

produced by arc-shaped permanent magnets radially magnetized," *Progress In Electromagnetics Research*, Vol. 95, 309–327, 2009.

22. Ravaud, R., G. Lemarquand, and V. Lemarquand, "Magnetic field created by tile permanent magnets," *IEEE Trans. Magn.*, Vol. 45, No. 7, 2920–2926, 2009.
23. Ravaud, R., G. Lemarquand, V. Lemarquand, and C. Depollier, "Magnetic field produced by a tile permanent magnet whose polarization is both uniform and tangential," *Progress In Electromagnetics Research B*, Vol. 13, 1–20, 2009.
24. Ravaud, R. and G. Lemarquand, "Discussion about the magnetic field produced by cylindrical halbach structures," *Progress In Electromagnetics Research B*, Vol. 13, 275–308, 2009.
25. Blache, C. and G. Lemarquand, "New structures for linear displacement sensor with hight magnetic field gradient," *IEEE Trans. Magn.*, Vol. 28, No. 5, 2196–2198, 1992.